Collapsing method for detailed recognition of seismogenic structures activated during underground mining.

Andrzej Leśniak[1], Elżbieta Śledź[1], and Katarzyna Mirek[1]

[1]AGH University of Science and Technology, Poland

Corresponding author: Elżbieta Śledź (esledz@agh.edu.pl)

Key Points:

- Seismicity induced during underground excavation indicates active emission zones.
- The collapsing method increases the resolution of mapping active seismic structures.
- Events in collapsed seismic cloud form the structures of rejuvenated fracture systems.

Abstract

In rock mass disturbed by mining activity, distortions in the stress balance may lead to seismic energy being emitted in rejuvenated seismogenic structures. One way of increasing the imaging resolution of these seismically active structures is through relocation, which itself can be achieved using the cloud collapsing method. This method partially eliminates perturbations in the location of seismic energy sources concerning the actual positions of these sources. It enables phenomena to be grouped into spatially ordered structures that can correspond to actual tectonic structures, such as fractures, fissures or faults. The article presents results of applying the collapsing method in mining seismology using cloud of tremors recorded during mining activity at one of the coalfaces in the Bobrek hard coal mine. The relocation procedure was applied to all the foci of tremors recorded during mining activity on face 3/503 between 04.2009 and 07.2010. In the relocated point cloud two types of linear structure responsible for generating tremors are distinguished: structures directly related to mining activity and structures associated with local tectonics. The location of the separated structures of the first type corresponds to the range of coalface 3/503 and the shafts delimiting earlier mined seams 507 and 509 located below. The isolated structures of the second type, with almost vertical orientation, are associated with existing zones of discontinuity that become seismically active as a result of mining activity. The identified structures lie near the biggest tremors recorded, which is evidence that these structures may correspond to real discontinuity zones.

1 Introduction

Underground mining of mineral resources (e.g. hard coal) or energy resources (e.g. crude oil, natural gas or geothermal energy) leads to changes in stress distribution in mining areas. These changes can disturb the stress balance and trigger dynamic phenomena in the form of seismic tremors of varying degrees of energy.

In the case of underground hard coal mining, a number of studies have noted the bimodal distribution of seismic energy(Gibowicz and Kijko, 1994; McGarr, 2000; Stec, 2007) which in general indicates two types of seismic phenomena associated with mining. The first type includes low and medium energy seismic tremors, which most often occur in the immediate vicinity of longwall faces or exploited chambers, usually as a result of mining activity. A characteristic feature of the mechanism behind these phenomena is the high share of non-shear components. The second type comprises medium and high energy phenomena associated with the renewal of old fractures and faults. They assume the form of tremors whose mechanisms are dominated by shear components. Their location is closely connected with the position of renewed seismogenic structures and may be located at a greater distance from coalfaces than the first type of phenomenon.

In many underground mines, including the Bobrek hard coal mine in southern Poland that is described in the article below, both categories of seismic events occur. Numerous phenomena directly induced by the fracturing of the rock mass occur in areas of mining activity and in the case of this mine are concentrated above the mind coal seam or directly below it. The sources of the second group of phenomena recorded during the course of mining activity are located significantly (over 500 m) below the exploited coal seam. Due to the mechanism of their sources, these phenomena are mainly associated with a fault network whose existence is postulated based

on tectonic and structural studies as well as on the genesis of individual geological structures. Their existence and location can only be inferred indirectly from seismic emissions.

The article attempts to determine the structures responsible for the generation of seismic phenomena in the Bobrek mine. For this purpose, the authors employed a method that involved collapsing a cloud of seismic sources in seam 503 as well as isolating active microtectonic structures (e.g. fissures and fractures) located in this area. The collapse is performed in the direction of local density centers of a cloud of seismic sources to increase the latter's resolution to map the structures responsible for the generation of seismic phenomena(Jones and Stewart, 1997). As the research shows, this method allows phenomena to be grouped into more spatially ordered structures such as lines or planes. These may correspond to actual tectonic structures such as fractures, fissures or faults.

First, the author will discuss the geological structure in the Bytom Basin area in which the Bobrek Coal Mine is located, together with the structural and geomechanical factors that contribute to high seismic activity both in this and in neighbouring areas. This will be followed by a description of the collapsing method applied to the seismic sources along with an example illustrating its effectiveness. Due to the significant impact that seismic emission location errors have on the collapsing procedure, the authors also addressed the problem of identifying errors in the location of emission sources recorded during the advance of the coalface. In the next part of the article, the author presents data recorded during the mining of seam 503 as well as the results of their relocation following the application of the collapsing procedure. Based on the above the next section identifies structures with a simple, linear geometry that is responsible for generating some of the tremors. These results were then set against the earlier results of seismicity studies in this area. In the discussion concluding the final chapter, the author presents the benefits of the analyzed method in studies of mining-induced seismicity, as well as their limitations.

2 Geological structure and seismicity in the area covered by the study

The occurrence of mining tremors depends on many factors, including the geological and tectonic structure, the location of the coalface, and past exploitation. The interaction of these factors has a significant impact on the formation of tremors.

The Bytom Basin forms a wide trough along a W-E axis and constitutes part of the Paleozoic Variscan structure which has been cut up by numerous faults. The Bytom Basin is an asymmetrical and relatively shallow trough with a complex structure. Its axis runs latitudinally from West to East near the north-eastern flank. As a consequence, the layers in this flank have quite steep angles of collapse which range from 8 to 20 degrees, while in the southern flank they do not exceed 3 degrees. The complex structure of the basin is additionally disturbed by a network of faults, mainly running in NW-SE direction and perpendicular to them, the planes of which have different projections and angles of inclination. Large faults with throw values of between several meters and almost 300 meters are accompanied by a network of smaller faults with throw values ranging in size from several dozen centimeters up to approximately 20 m.

Carboniferous formations in the studied area reach a thickness of up to 550 m and contain numerous coal seams of varying thickness, up to a maximum of 12 m. A characteristic feature of the carboniferous period is its cyclical structure expressed by the alternating occurrence of sandstone, silt, claystone, conglomerates, and coal. These rocks differ in terms of their elastic properties and compressive strength. For example, sandstone has higher strength parameters than claystone and coal. One additional factor that has a decisive impact on the geomechanical properties of rocks is tectonics in all its forms (faults, joints, cleavage, and other inhomogeneities), which significantly reduces the strength of the rock massif.

In the past, the Bytom Basin had been an area of very intensive hard coal mining. In the 1990s production was scaled back significantly and exploitation of zinc-lead ore was brought to an end, as a result of which the rate of subsidence decreased together with the number of high-energy tremors. However, this is still an area where mining activity continues to have a negative impact on the surface and continues to generate seismic tremors.

The propensity for rock bursts to occur in a rock mass depends on the geomechanical properties of the rock. It was found, for example, that an area was particularly susceptible to tremors when thick benches of strong rock, such as sandstone or mudstone are located in the vicinity of a deposit(Goszcz, 1999). Another influential factor is old tectonic stresses occurring in the rock, which have led to changes in geomechanical properties, increasing or decreasing their propensity for rock bursts.

In the Upper Silesian Coal Basin, tremors caused by coal mining activity are concentrated in several areas, one of which is the Bytom Basin. The susceptibility of a rock mass to rock bursts is explained in different ways. Studies have revealed a close relationship between mining activity and low energy tremors, while more powerful tremors are associated with the tectonics of the Upper Silesian Coal Basin. The widespread occurrence of rock bursts in the Bytom Basin was initially explained as being the result of increased stresses in the syncline folds. However, it seems that the higher risk of rock bursts in these basins is due to the compaction of rocks, whereas in the past all three principal tectonic stresses were compressive in character(Goszcz, 1999).

Stec proposed a general classification of the seismic tremors in this area, which involved dividing them into three groups(Stec, 2007, 2009).The first group consists of tremors with a slipping and shearing foci mechanism. Tremors of this type occur during progressive mining as a result of fractures in the seam of thick and compact rock complexes with high rigidity and strength parameters. The second group consists of tremors characterized by foci with a non-shearing mechanism. Such tremors are located directly in the coal seam and in the vicinity of active coalfaces. The third group comprises "regional" tremors, characterized by the highest energy, which usually occur far from areas of active mining activity. Their foci have a slip mechanism that is normal or reversible in character. The most common cause of these events is the interaction of tectonic and residual stresses existing in the analyzed area with mining-induced stresses.

The exploitation area of the Bobrek mine encompasses the region of the Bytom Basin (see Figure 1). This is one of the three areas where the majority of mining tremors were recorded,

including high energy tremors with magnitudes of up to 4.0. During the mining of face 3 in seam 503 (3/503), the first tremors were observed in April 2009. The area remained seismically active until July 8, 2010. Most of the recorded tremors were low energy tremors. However, four higher magnitude tremors were also registered: 2.9 (20.05.2009), 3.7 (16.12.2009), 3.0 (5.02.2010) and 2.8 (11.03.2010).

Marcak and Mutke (2013) analyzed tremors recorded by mining seismological stations during mining of coalface 3/503. The authors concluded that tectonic stresses were of key importance in the distribution of seismic tremors. It was also observed that higher energy tremors began to occur as the coalface reached the axis of the Bytom Basin. The hypocentres of high energy tremors were located at a depth of 300 m to 800 m below the mined seam. At the same time, it was noted that once they had passed through the Bytom Basin the energy produced by these tremors weakened and the depth of their hypocentres also decreased. The latter still occurred below the mined seam, but at a depth of less than 200 m. Furthermore, the authors showed that high-energy tremors occurring in the vicinity of the Bytom Basin had a different character to the phenomena typical of the Upper Silesian Coal Basin. The mechanism of these phenomena is associated with slipping in reverse faults, and the nature of the phenomena indicates a relationship between them and tectonics.

These results were partially confirmed in the work of Kozłowska et al.(2016). In this article, the authors analyzed a 3.7 magnitude tremor that occurred on December 16, 2009, during the course of mining coalface 3/503. The tremor mechanism indicates a reverse fault with an almost vertical plane. Numerical models that took into account current and past mining activity indicate that the phenomenon is associated with tectonics. However, mining activity affected a change in the stresses present in the local tectonics, which in turn triggered a fault process or the formation of a new fault on the weakening plane.

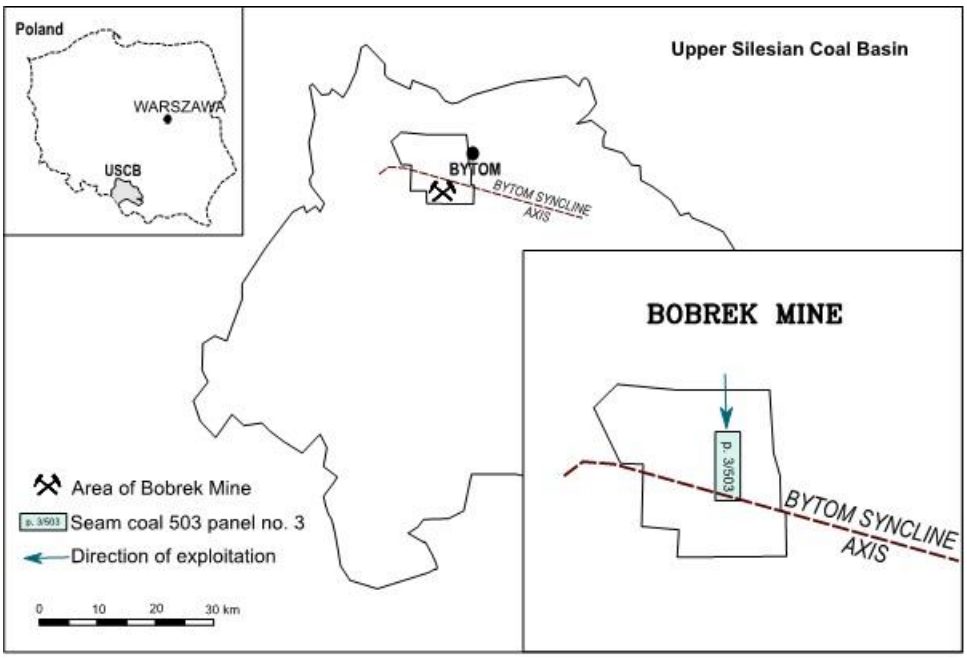

Figure 1. Location of the Bobrek mine area against the background of the Upper Silesian Coal Basin.

3 Theory

To ensure more precise imaging of seismically active microtectonic structures based on registered seismic emissions, the authors proposed applying the collapsing method(Fehler et al., 1997; Jones and Stewart, 1997; Phillips et al., 1997). This is one of the techniques used to help identify the microtectonic structures responsible for the emission of some of the tremors accompanying the stimulation and exploitation of hydrothermal reservoirs and hydrocarbon deposits.

The collapsing method differs from other methods employed to locate seismic sources in the way it uses information regarding errors in the location of hypocenters of seismic events. Classical approaches, such as the P-time method(Geiger, 1912), or techniques that take into account not only the arrival times but also the direction of seismic rays(Leśniak, 2015) minimize the functional describing the differences between the measured times and/or directions and their values calculated based on the assumed velocity model. For minimization purposes, it is the linear version of this functional that is most often performed. In this case, a location error is represented as an error ellipsoid(Havskov and Ottemoller, 2010. Its spatial orientation depends on the relative location of the emission source and sensors, and the volume illustrates the level of confidence with which the emission source is found inside the ellipsoid. The spatial distribution of a location error only assumed the form of an ellipsoid if the minimized functional is linearised. When other methods are employed to determine the minimum functional (e.g. the Monte Carlo simulation methods, for example in the MCMC variant(Mosegaard and Sambridge, 2002)), location error distributions are often not ellipsoidal in shape(Leśniak and Pszczoła, 2008). They depend to a great extent, on both the configuration of the sensor network and the quality of registration as well as on the specific location method used(Rudziński and Dębski, 2013).

In the case of the source collapsing method, the location error is used not only to determine the location accuracy of a particular emission source but also to determine the course of the relocation of emission sources. The relocation (referred to in the collapsing method described below) of sources takes place within the boundaries of the error ellipsoid, and thus the new distribution of the sources (following the collapsing process) may reflect the actual spatial distribution of the foci of tremors undisturbed by the location error. This distribution is usually characterized by greater regularity and less spatial dispersion(Jones and Stewart, 1997). There are several variations of the original collapsing method. Asanuma et al. proposed a modification of the first version of the collapsing method, where structure of the cloud depends on the distribution of locations within confidence ellipsoid(Asanuma et al., 2001). Additionally, in the modified collapsing procedure location movements depend on the dimensionality on the estimated original structures. In other publications, Asanuma et al. presented (Asanuma et al., 2005, 2008) another modification of the collapsing method that uses mutual coherency of waveforms and to establish the similarity of events. Here in the paper we use the original collapsing method.

In a rock mass whose stress distribution has been disturbed by mining activity, a seismic emission is mainly associated with slippage on rejuvenated faults and fractures as well as with the formation of new fractures. The former constitute the main network of fractures while the latter form the network of micro-fissures. Slippage and expansion of the main fracture network is

the source of some of the registered events spatially distributed along with systems with a relatively simple linear structure, e.g. planes or straight lines. The spatial distribution of other phenomena is more chaotic in character and greatly depends on the mineral composition and texture of the particular rock.

Every measurement involves some level of error. The location of emission sources is also erroneous, which causes perturbation of localized sources in relation to the actual positions of these sources and blurs the undisturbed image of the emission cloud. The purpose of collapsing is to limit at least partially such blurring and reduce perturbation. To this end, the sources are relocated and are shifted towards local emission densities.

The perturbation of the actual location of an emission source occurs randomly. This means that the total shift vector, i.e. the sum of three orthogonal vectors oriented in line with the directions of the individual axes of the coordinate system, is random. It can be assumed in this case that the components of the displacement along these three orthogonal directions have a normal distribution with individual mean values and dispersions. It can be argued that if each of these distributions is standardized, the total degree of displacement will be random in terms of direction and value defined by χ^2 distribution with three degrees of freedom(Evernden, 1969). Therefore, the closer two points are actually located, the greater the chance (in a statistical sense) that the distance between them as a result of perturbation will increase more in relation to the original distance than will the relative distance of points positioned further apart.

Let us consider the example presented in Figure 2, in which the location of real seismic sources, uniformly distributed on a straight line Figure 2A, has been affected by perturbation These points are then dispersed in random directions at a random distance. Each of the X, Y and Z coordinates of the relocation vector is a random variable and has an identical normal distribution with a mean value of zero and a variance of 0.1. Figure 2B presents the points cloud modelled on this basis, which shows the distribution of emission sources after perturbation.

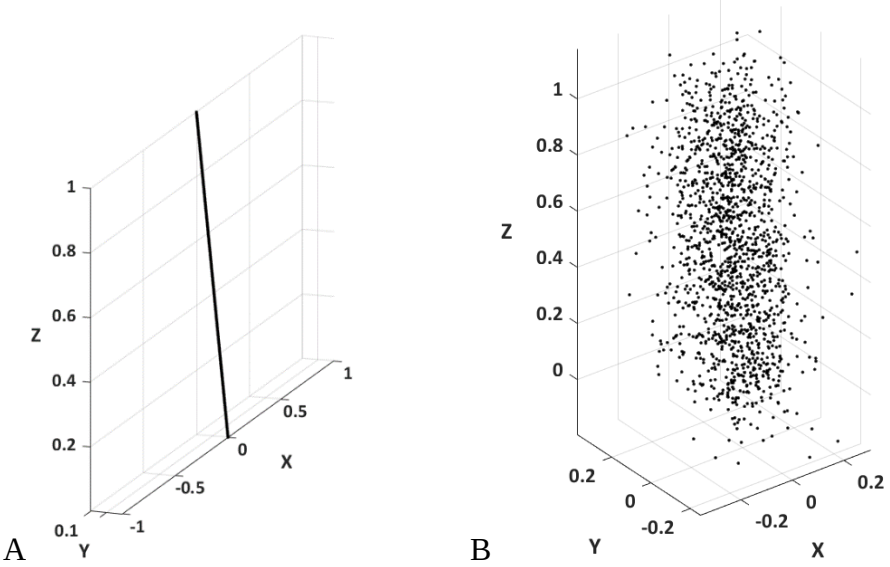

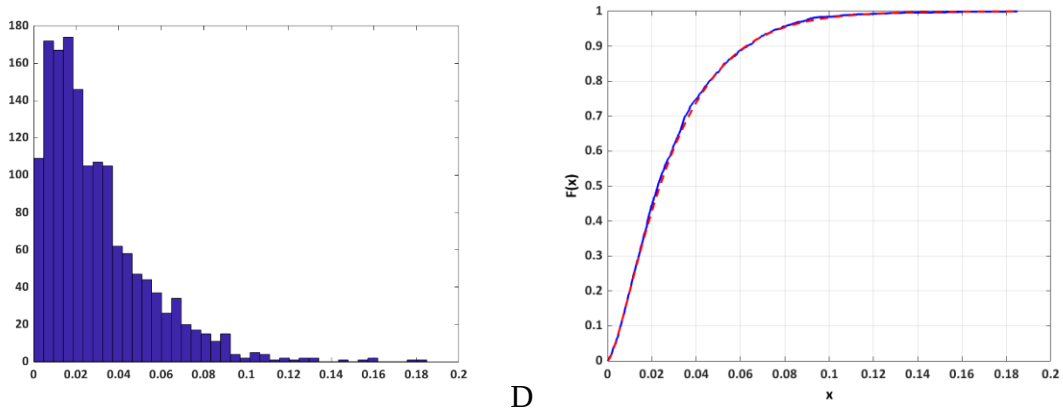

Figure 2. Population of points arranged on a straight line before A) and after B) perturbation of their positions. C) a histogram of the displacement vector length during the perturbation process, D) a comparison of the distribution function of the empirical distribution (red curve) and the theoretical distribution (blue curve) prepared for the needs of the Kolmogorov-Smirnov test.

Figure 2C presents an empirical histogram of the length of the displacement vector obtained during perturbation. Because each vector coordinate of a perturbation is a random variable with normal distribution, the square of the vector length of the perturbation, being the sum of the squares of the vector coordinates of the perturbation with normal distribution, has χ^2 distribution with three degrees of freedom. This becomes clear after performing the Kolmogorov-Smirnov statistical test (K-S test). This test compares the empirical cumulative distribution function with the theoretical cumulative distribution function of χ^2 distribution. Figure 2D presents both cumulative distribution functions. The K-S test, in this case, shows the compatibility of both kinds of distribution.

The collapsing procedure is designed to reduce the perturbation of emission source locations. It involves gradually shifting emission sources towards local source densities. What is important to note is that the relocation of each emission source takes place within its error ellipsoid, in relation to which the source's location was established. The procedure is shown in Figure 3.

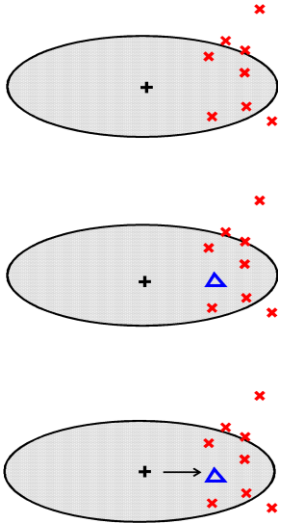

Figure 3. Image showing the relocation of seismic emission sources towards local emission source densities.

For each localized hypocenter:
• the localization error ellipsoid (black cross) is calculated for a given confidence interval as well as all phenomena whose hypocenters lie within this ellipsoid
• the center of gravity is determined for the points within the error ellipsoid (blue triangle)
• the hypocenter of the analyzed phenomenon is shifted towards the center of gravity (the ellipsoid remains in its original position)

In a particular iteration, positions from the previous iteration, which have not been updated in the current iteration, are taken into account as successive hypocentres are displaced. Shifted hypocentres create a new set of locations. The entire relocation procedure is repeated in the same way for each subsequent iterative step until the translation population assumes the form of a chi-square distribution with three degrees of freedom. The procedure is checked using the Kolmogorov-Smirnov test (K-S test) assessing the compliance of the empirical distribution with theoretical distribution χ^2. As was mentioned above, in subsequent iteration cycles the error ellipsoids do not change their position.

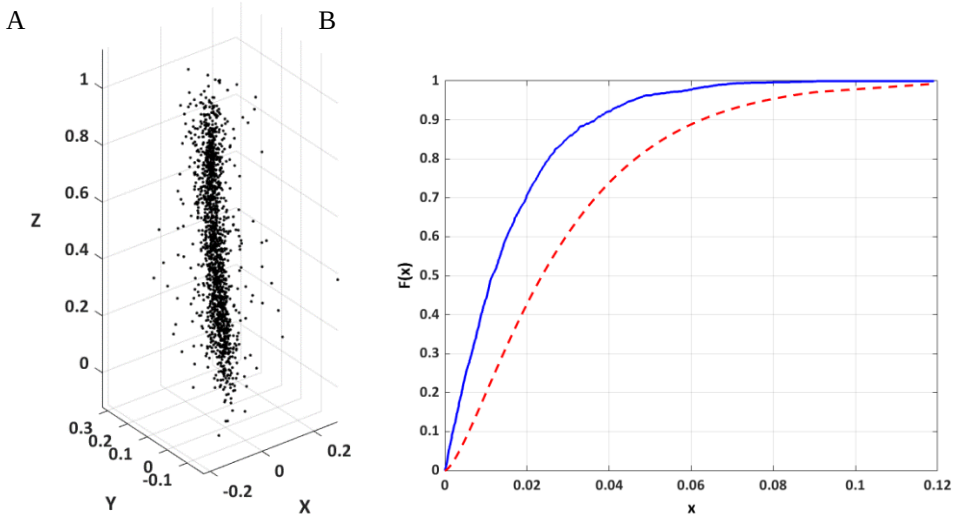

Figure 4. A) The population of points after the first stage of the relocation operation. B) A comparison of the empirical distribution function (red curve) with the theoretical distribution (blue curve) after the first collapsing step for the needs of the Kolmogorov-Smirnov test.

Figure 4 A) presents the points population after the first relocation step. As can be seen, the distance between points has been reduced. The empirical cumulative distribution of the relocation vectors in the first collapsing stage is represented in Figure 4B by a dashed red curve. It is compared in the Kolmogorov - Smirnov test with theoretical distribution. χ^2. As can easily be seen, the two distribution functions are very different. Also, the K-S test result is negative. As has been noted above, if the hypothesis is rejected, the next relocation step is performed and the test is carried out once more. The procedure is repeated until the total distribution of displacement length achieves distribution χ^2 (thus adopting the hypothesis that both distributions are compatible) or when no progress is observed in matching both distributions in subsequent

iterations. In turn, Figure 5A and 5B show the distribution of sources after the second and third relocation steps along with the empirical distributions of total displacements against the backdrop of theoretical distributions.

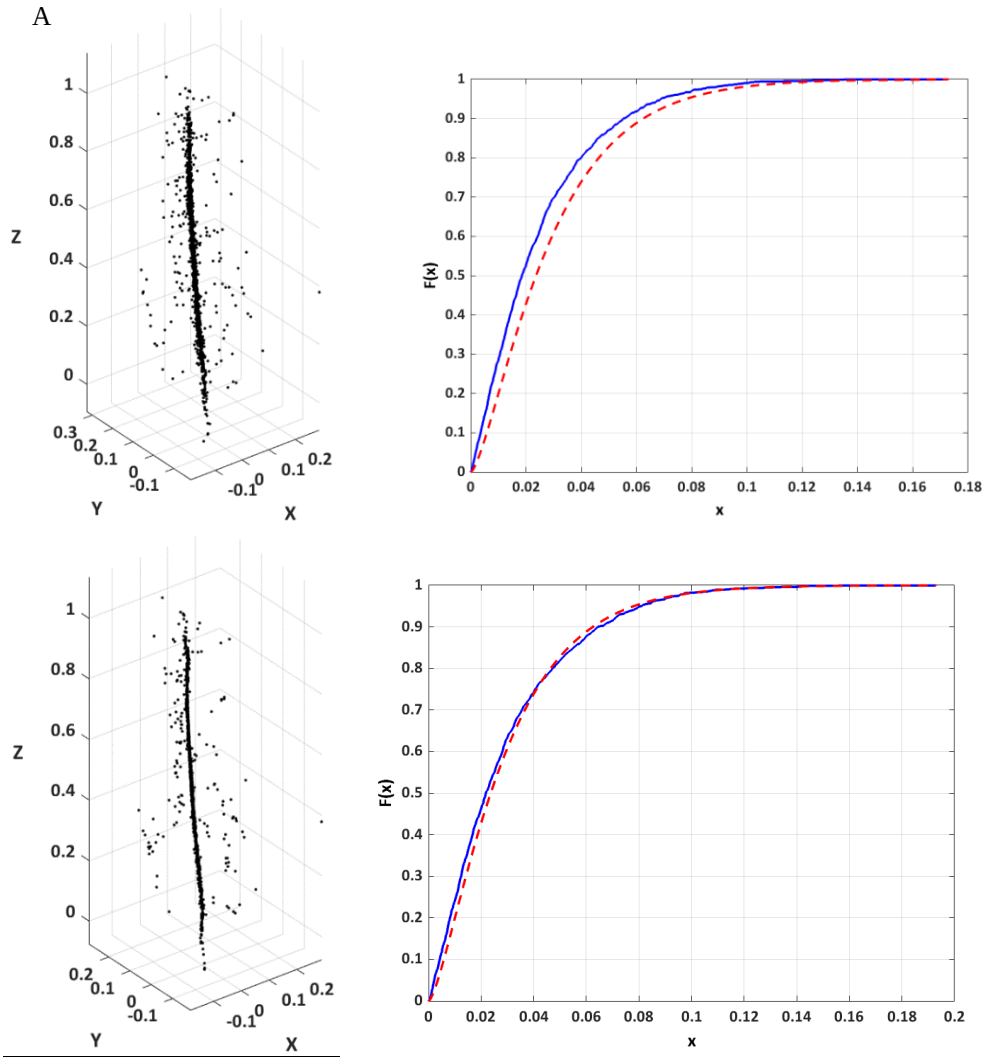

Figure 5. The second A) and third (final) B) relocation stage. The left column presents the location of sources following relocation and the right column compares the empirical and theoretical cumulative distribution functions after each subsequent.

In the case of the example presented above, after the third step, most sources had already been relocated to a straight line, the location of which reflects the original location of the sources. It is also worth noting that not all the points were relocated. If for a given source the error ellipsoid with which it has been located is insufficient and does not include other sources, then the source is not relocated. The size of the ellipsoid is related to the adopted confidence level. In this case, it was assumed to be 0.95, which means that there is a 0.95 probability that the source is located within the error ellipsoid.

4 Data

The Laboratory for Monitoring Mining-Induced Seismicity (LMMIS) conducted research on local seismicity caused by underground coal mining in the Bobrek mine. These studies were part of the IS-EPOS project(https://tcs.ah-epos.eu/#episode:BOBREK, accessed January 2020). Within their framework, a total of 2995 tremors were recorded and located. They were registered as a result of the exploitation of coalface 3/503 in the period between April 2009 and July 2010. The hypocenters of these tremors occurred at various depths, ranging from 300 m below ground level to more than 2300 m below ground level. The local magnitude of these events ranged between 0 and 3.7. The most powerful tremor had a local magnitude M_L = 3.7 occurred on December 16, 2009. This mining-induced tectonic event was associated with the local tectonic structure of the Bytom Syncline(Kozłowska et al., 2016).

The Bobrek mine seismic network consists of 27 geophones with a recording band above 1 Hz. It is composed of 21 uniaxial and 6 triaxial geophones, all with a sampling frequency of 500 Hz. Most are located at the level of the exploited seam (approximately 750 m below the surface), two at sea level and one at surface level. During the analyzed period, individual geophones were serviced and repaired. As a consequence, only those geophones that were operational on the day a particular event occurred were included in the location.

The locations were determined using the classical method for locating tremor sources based on uniaxial (vertical) sensors and triaxial sensors according to the registration times of the first seismic signal. An approximate model of medium velocity in the area of seam 503 was adopted, for which the velocity of longitudinal wave propagation (used for localization) was 3850 m / s. The location of geophones, along with the location of the sources of all registered seismic tremors, is presented in Figure 6.

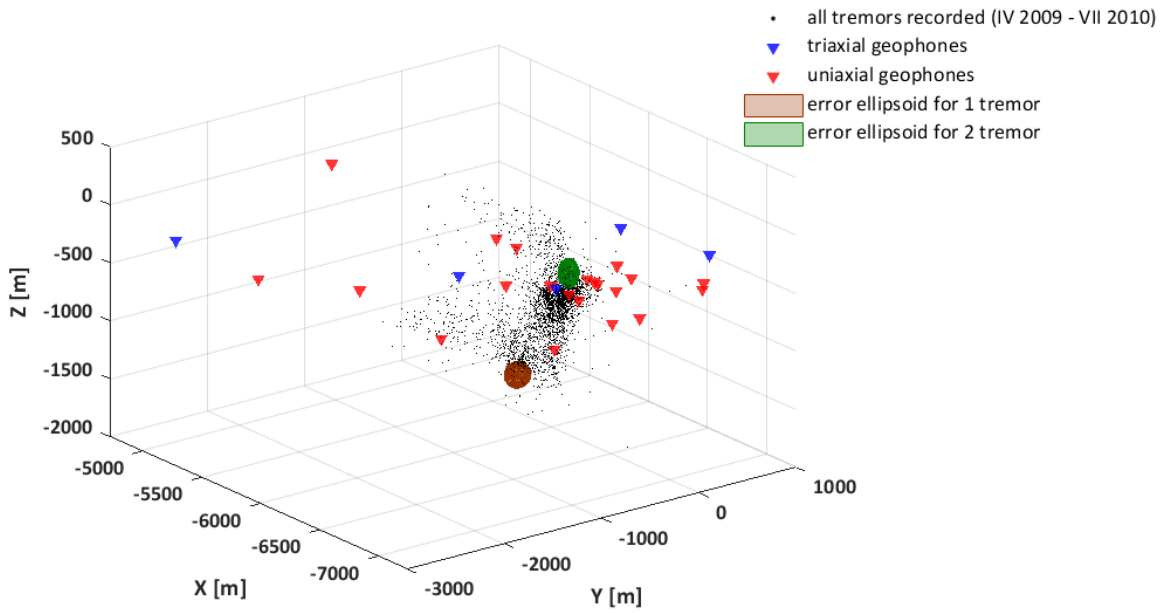

Figure 6. Seismic network of the Bobrek mine with tremors registered between April 2009 and July 2010. Uniaxial geophones are marked with red triangles and triaxial geophones with blue triangles.

Figure 7 features a histogram showing the seismic activity for each month. This histogram indicates that seismic activity changed during the period in which the mine was in operation. From December 2009 to May 2010, the number of tremors increased significantly, especially when compared to the months preceding this increase. This coincided with the moment when the active coalface crossed the Bytom basin axis.

The same figure shows the percentage of seismic phenomena whose sources were located below seam No. 503 in relation to the total number of such events. Face 3 of this seam lies at a depth of approximately 700 m below the surface and, as such, the majority of the tremors were generated below this depth and only a small (roughly 10%) number occurred above. The number of tremors below the seam was calculated by taking into account the depth of the coalface at the end of each period. Most of the tremors occurred below seam 503. During this period, a small number of tremors were also recorded in the seam roof.

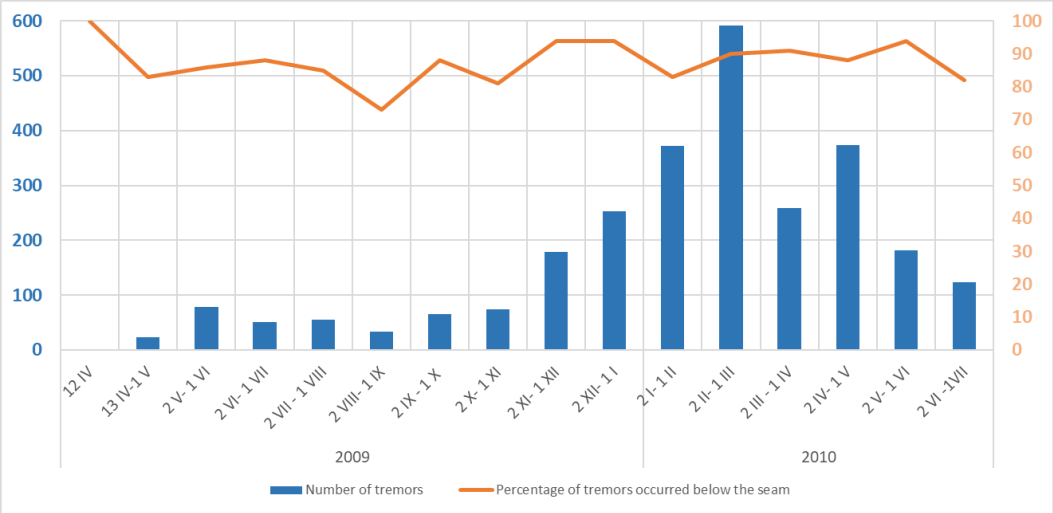

Figure 7. Number of tremors for each month between April 2009 and July 2010

As has already been noted(Marcak and Mutke, 2013) the highest energy tremors took place 300-800 m below the mining level and were located at a short distance from the axis of the Bytom Basin.

The key to implementing the collapsing procedure is determining the location ellipsoid error for a seismic event. The orientation of the error ellipsoid is determined by the spatial configuration of the sensors in relation to the source location. The size of the ellipsoid is established by the partial errors in the measured parameters. To determine the error ellipsoid, it was assumed that the error in the time of the P wave was, depending on the signal quality, 4 ms. However, greater accuracy was achieved with good quality signals, dropping to as low as 2 ms. The sensor location error parameter was estimated at 0.1m. In addition to the two types of error mentioned above, the magnitude of the location error is also affected by the simplified velocity model for the center of seismic wave propagation, both in terms of the inaccuracy of the geometric structure and the variable speed values. Assuming that the errors are random with normal distribution and that the measurement is not burdened with a permanent error caused by, for example, defective measuring equipment or significant differences in conditions around the ellipsoid sensors, the location of an emission source can be defined as follows(Jones and Stewart, 1997; Leśniak, 2015):

$$\sigma_s^2 = \sigma^2 (G_s^T G_s)^{-1} \chi_3^2(\alpha) \quad (1)$$

where $G_s$is a matrix containing partial derivatives of spatial residues,σ^2 constitutes the variance of the data while $\chi_3^2(\alpha)$ is the chi square distribution value with three degrees of freedom for significance level α (in our case 99.5%). Sample error ellipsoids for the location of the foci of two tremors occurring at different depths at the adopted significance level are shown in Figure 6. The distribution of the tremor cloud is shown in monthly time intervals - before and after collapsing, together with the current position of the active coalface in Figure 8 A) - O) and Figure 10 A) - O). The coalface progressed at an average pace of 50 m from month to month. In each sketch, the blue line indicates the position of the coalface at the beginning of the selected

time interval, and the red line the position at the end. The mining works proceeded from north to south perpendicular to the axis of the Bytom basin. The axis of the Bytom basin was crossed in April 2010, two months before mining of the seam came to an end.

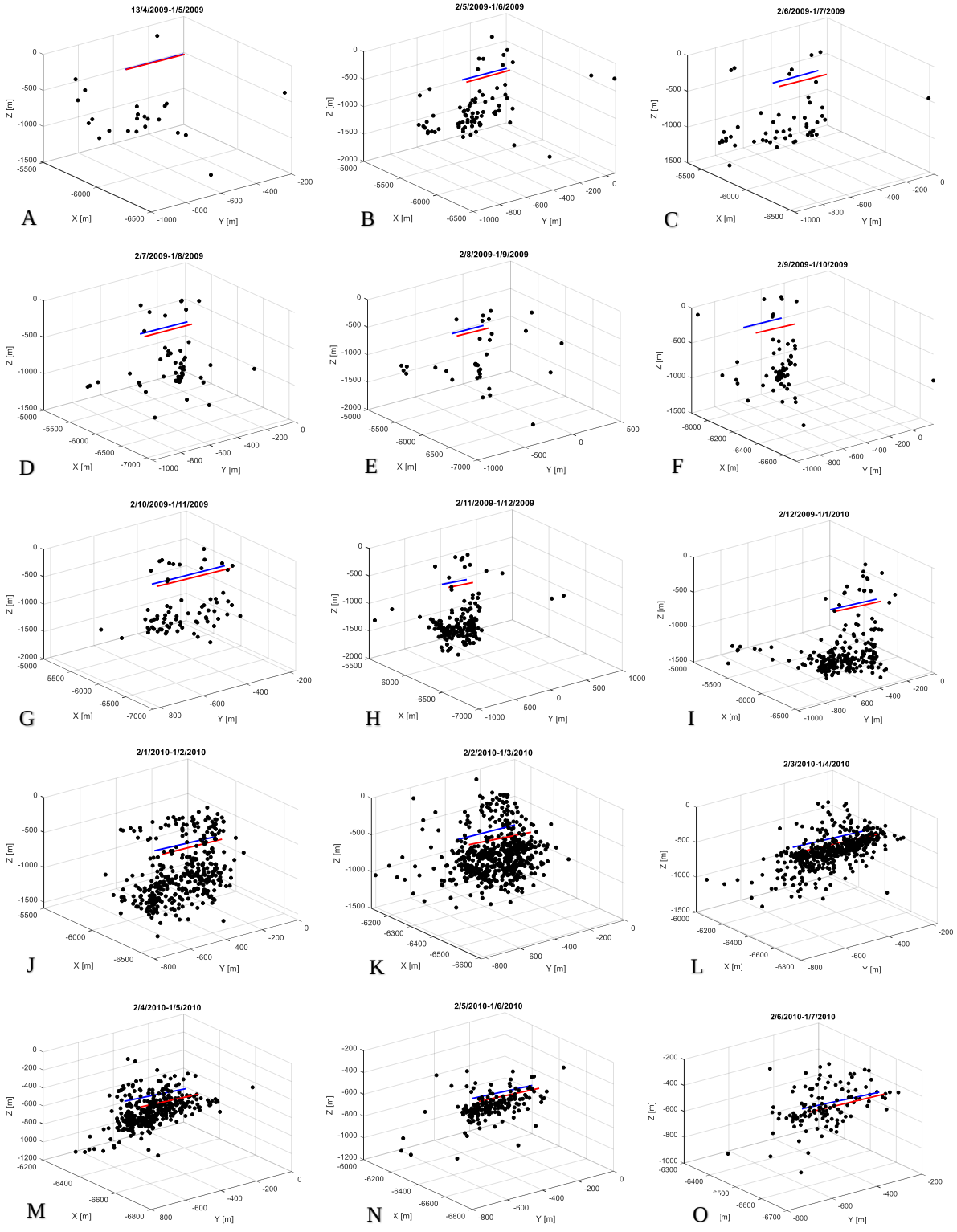

Figure 8. A-O Location of the point cloud in monthly intervals along with the current position of the coalface at the beginning and end of the interval

It can easily be seen that in the early months of mining activity, seismic emissions were relatively low and occurred mainly between 500 and 1000 meters below the seam. In the next six months of mining at the seam, the emissions were similar to one another in terms of both intensity and the average depth of the source location. Starting from September 2009, there was a significant increase in emission intensity as well as a gradual decrease in the location depth of the sources. In the last two months of mining activity (sketches 8N and 8O), emissions occurred relatively close to the seam, where coal was being mined.

5 Results

All the foci of seismic emissions recorded during the analyzed time period underwent relocation procedure. As was described in section 3, an error ellipsoid was calculated for each source within which displacement towards a local density center was possible. The process was iterative in form, testing through repetition whether all displacements form a χ^2 distribution. As was mentioned above, the key to the relocation process is the size and orientation of the error ellipsoid. The orientation mainly depends on the spatial configuration of the seismic network and its size, in accordance with formula 1, as well as on the variance of the data and the confidence level used for the cut-off. A high degree of location accuracy (a relatively small error ellipsoid) does not allow for any significant displacement of localized sources. A lower degree of location accuracy (larger error ellipsoid) allows for larger displacements. The creators of the method suggest using relatively large values for the ellipsoid confidence level, arguing that a change from 2σ (95%) through 3σ (98%) up to 4σ (99.86%) does not significantly affect the collapsing results(Jones and Stewart, 1997). In turn, the data variance should be estimated on each occasion, as was discussed in the previous section.

First, the results of the collapsing procedure for the entire data set were presented. The location of the tremors in each iteration is shown in sketches 9 E-H. The compatibility of the theoretical and empirical distributions was checked using the Kolmogorov-Smirnov test in each iteration. The differences between theoretical and empirical distributions are presented in sketches 9 A-D. One can be observed that in subsequent stages the difference between the theoretical and empirical cumulative distribution function decreases. The procedure is carried out until the null hypothesis is achieved, i.e. when both distributions are compatible with each other. The size of the ellipsoid used for the calculations is 0.995. The statistical significance value (parameter p) was examined. In the first relocation step it was 0, and in the following steps: 6. 7507e-263, 5.0692e-44, 0.0062. In the 4 iterations, distribution compatibility was achieved within the assumed error.

Sketches 10 A-O show the post-relocation tremors registered in individual months of mining activity. A comparison of this data with the distribution of tremors before the collapse (sketches 8 A-O) shows that the number of sources involved in relocation increases as the active coal face

approaches the axis of the Bytom basin. This process can be observed by comparing the point cloud images for individual months in Figures 8 and 10 beginning from Sketches H to O. Here we can observe the collapse of the cloud into one-dimensional linear structures. These structures can generally be divided into two groups. The first comprises horizontal structures closer to the seam running parallel to the active coalface (e.g. sketches 10 L, M, N). The second consists of structures with an almost vertical course and located at a greater depth (as in sketches 10 E, H, I).

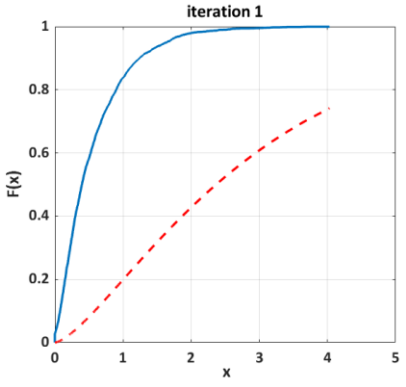

A

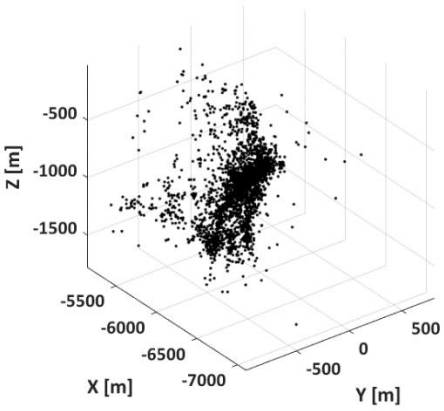

E

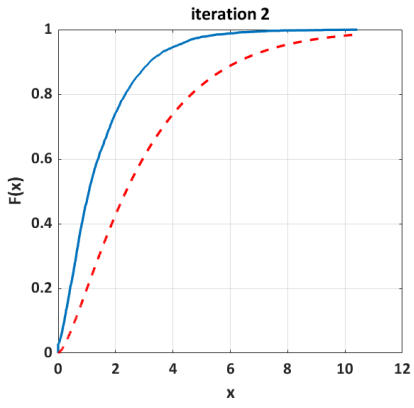

B

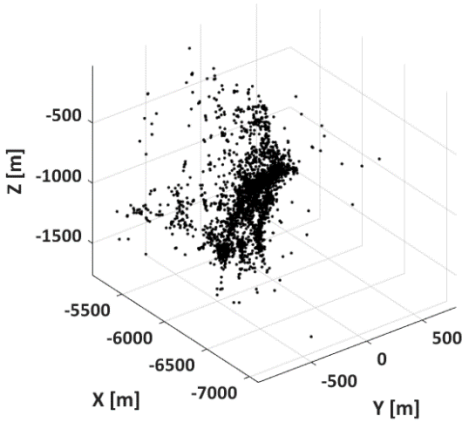

F

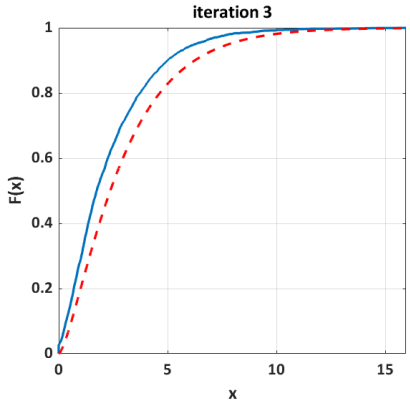

C

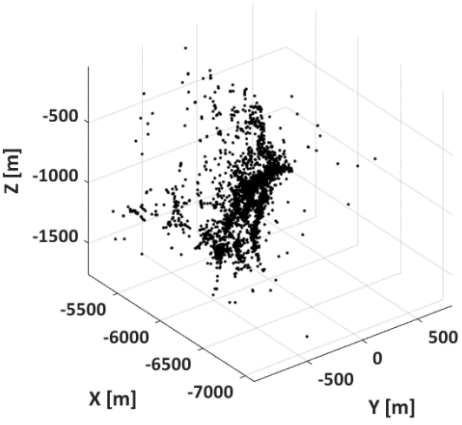

G

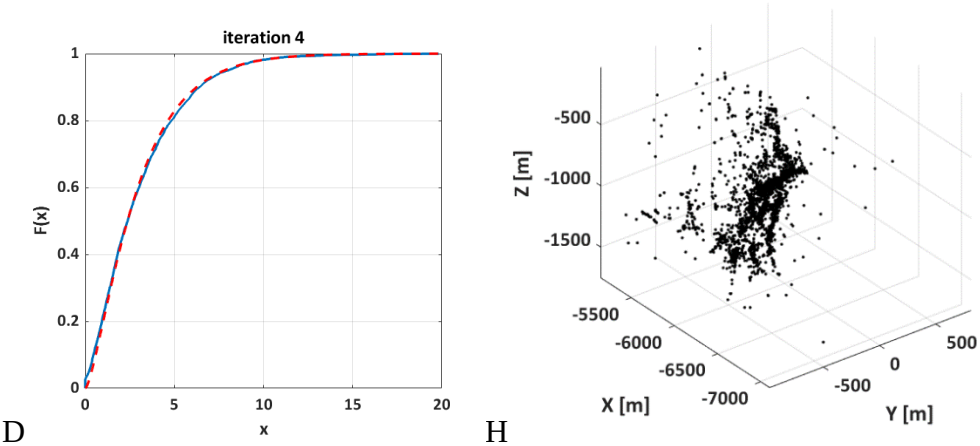

D H

Figure 9. A) - D) A comparison of theoretical and empirical distribution functions. The red dashed curve denotes the empirical distribution function while the blue dashed curve represents the theoretical distribution function. E) -H) locations of tremor cloud foci in subsequent iterations

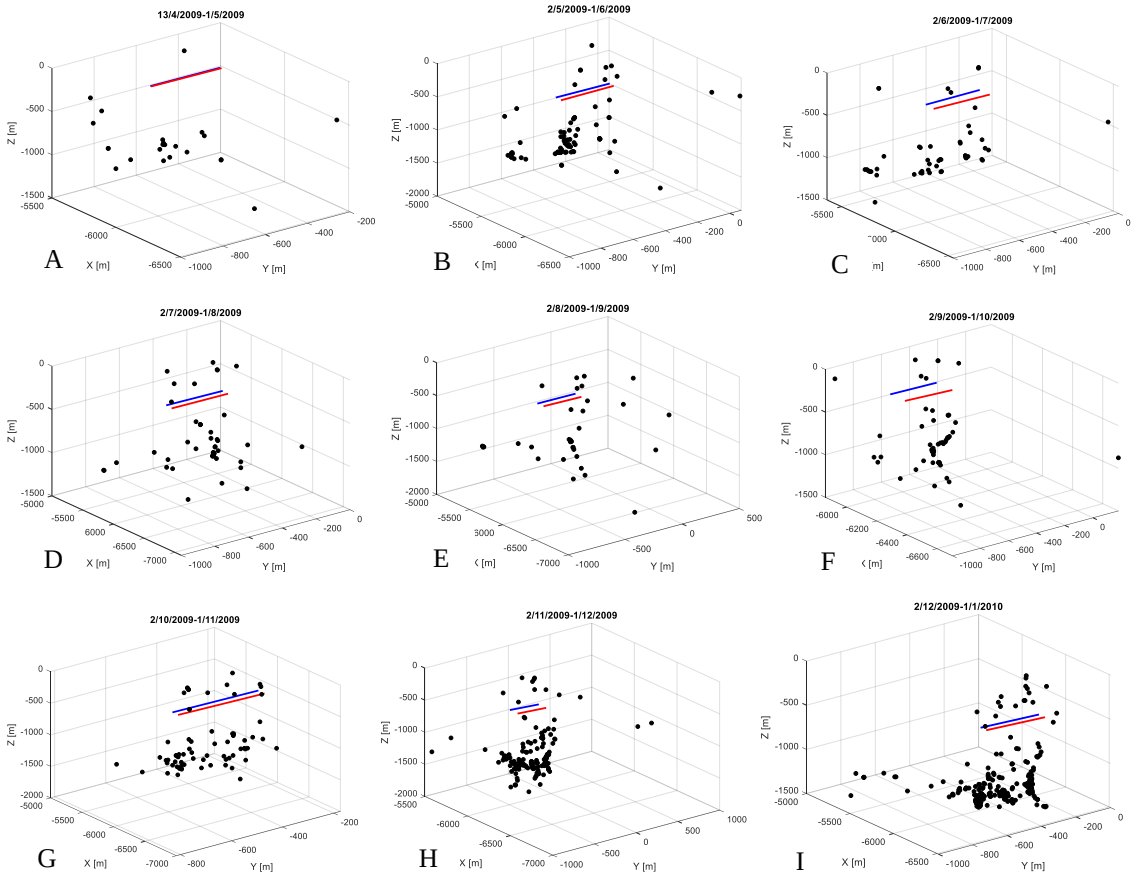

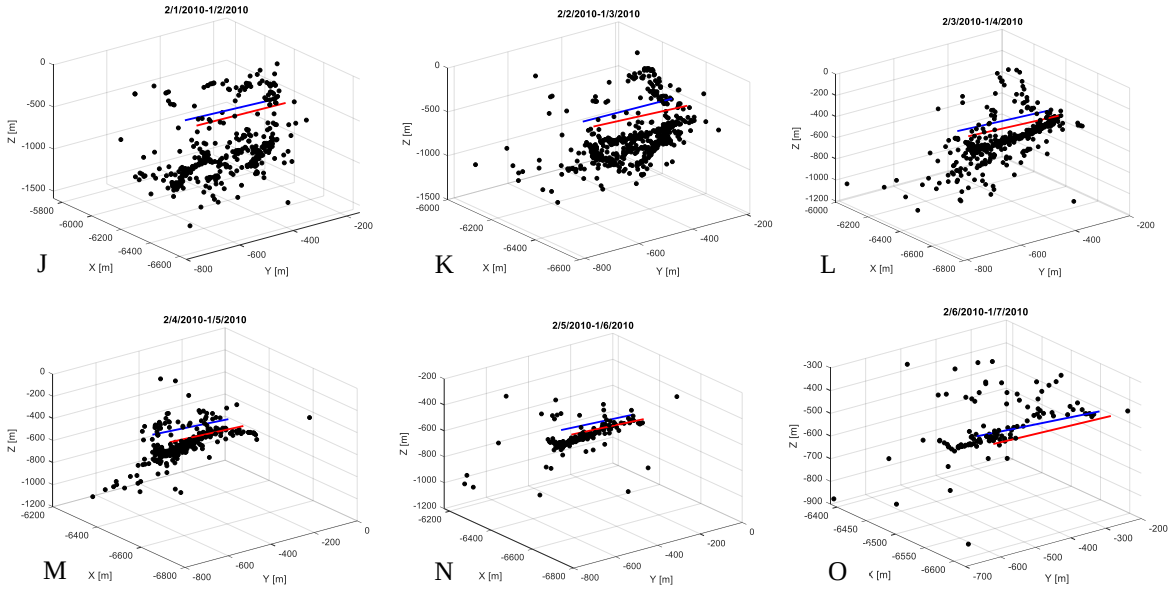

Figure 10. A) - O) Location of displaced point cloud via the collapsing method in monthly intervals along with the current position of the active coalface at the beginning and end of the interval.

Figure 11 shows the emission cloud following relocation set against the background of both seam 503 and two deeper, previously mined seams 507 and 509. Following the collapse of the sources, most phenomena were concentrated below the seam where mining activity was taking place (blue line) in the vicinity of the previously mined seams (lines green and orange). A specific image is likewise formed by the foci of numerous tremors grouped in narrow zones with a vertical or almost vertical course. They occur near the axis of the Bytom basin, the course of which is marked with red arrows. A relatively small number of tremors occurred above seam 503. One important trend to note is the sharp drop in the number of tremors that occurred once the basin axis was crossed, first above the seam and then below it.

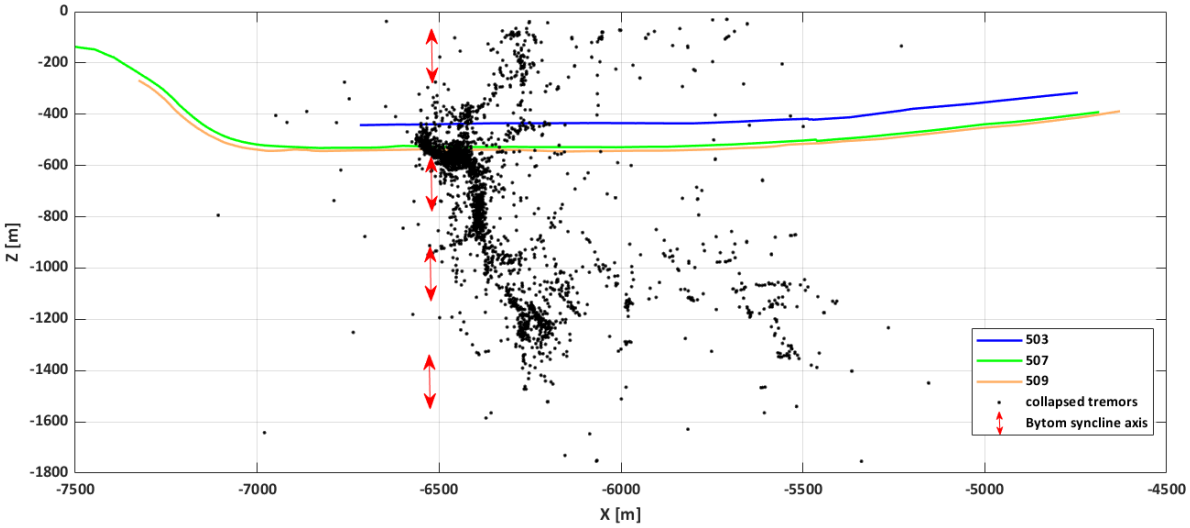

Figure 11. Vertical crossection of seam 503 and previously mined seams 507 and 509 located below along with the location of emission sources after relocation as well as the axis of the Bytom basin.

Generally speaking, following relocation the cloud representing the foci of tremors is more heterogeneous, as is manifested in the occurrence of local densities of various shapes. Most often they assume a shape similar to straight lines and planes with different orientations.

6. Interpretation

Based on the results presented above, an attempt was made to identify linear structures using a cloud of seismic tremors displaced by means of the collapsing method in the data set taken from the entire period of mining activity (Figure 12 A-B). The structures were identified with Matlab software, whose graphic interface allows for a 3D visualization of a cloud, rotation, and scaling. The goal was to identify distinct groups arranged along straight lines or on planes. Small structures were not marked, including those that were small in size and those containing a small number of points. This is because their location would have been largely subjective.

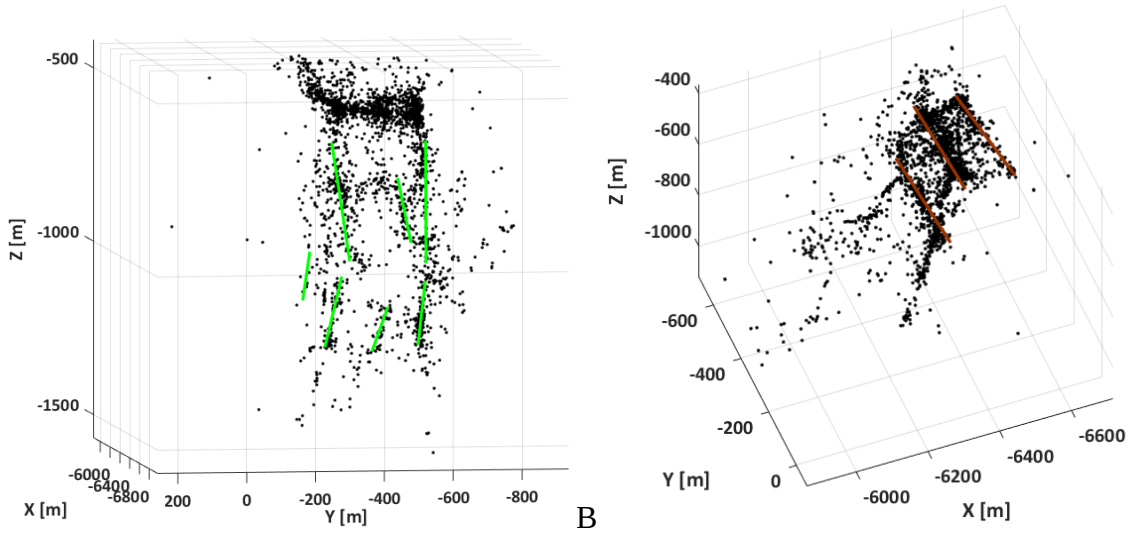

A B

Figure 12. Separated structures A) vertical and B) horizontal in the cloud after collapsing

The separated structures are associated with areas characterized by a rectilinear course with an above-average density of events. They are associated with real places of intensive seismic emission that run along fracture zones with weakened rock mass. Green lines with an almost vertical course can be interpreted as local tectonic discontinuities that have been activated as a result of mining activity. Their occurrence was previously postulated by Marcak and Mutke(2013) and was associated with the occurrence of flexures (monoclinal fold) in the Bytom basin. In basins of this type, we can expect the occurrence of fracture systems of varying scale with an almost vertical course and thus perpendicular to the axis of the basin and the selected seam(Li et al., 2018).The structures shown in Figure12 are characterized by a depth of occurrence of between 500 m and 1400 m ppm, i.e. they are located below the two exhausted seams.

The brown lines with a more or less horizontal direction run parallel to the active coalface and progress in tandem with its progress. Significantly, they occur deeper than exploited seam 503, namely in the immediate vicinity of exhausted seams 507 and 509. Figure 13 presents, against the backdrop of seams 503, 507 and 509, the location of the collapse cloud and the range of exploited face 3/503 as well as the location of the shafts delimiting the exploited faces of seams 507 and 509.

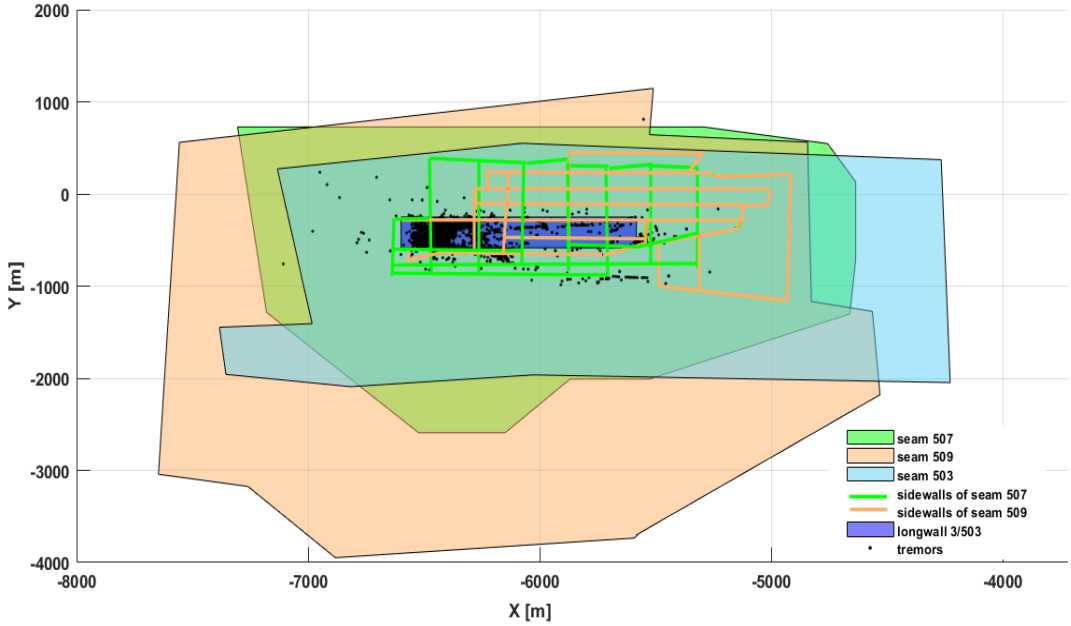

Figure 13. Flat projection of the boundaries of seams 503, 507 and 509, the range of exploited face 3/503 and the location of the shafts delimiting the exploited faces in seams 507 and 509. The black points show the location of the cloud of phenomena the following collapse.

The shafts of exploited seams (lines marked in green and orange) roughly demarcate the zones located below exploited seam 3/503, where the continuity of the rock mass was disturbed as a result of mining activity prior to the exploitation of seam 503. These disturbed zones were the site of an intensive seismic emission faithfully depicted by the spatial distribution of seismic emission sources (see Figure 13). The horizontal structures marked with brown lines in the cloud of phenomena in Figure 12 have similar positions and spatial orientations to the shafts of earlier exploited seams 507 and 509. Such compliance is very good for structures closer to seam 509.

As has already been noted in the case of mining-induced emissions, two types of seismic tremors are generally distinguished– mining-induced tremors and tremors of mining-tectonic origin(Stec, 2007). Mining and tectonic seismicity are caused by the interaction between, on the one hand, mining activity, both current and in the past, and, on the other, locally existing seismogenic zones such as faults as well as areas affected by mining activity. Mining seismicity is associated with events located near active mining excavations. The vertical structures isolated from the emission cloud were linked above with relatively large fracture zones, which in turn are connected with the flexure of the Bytom basin. These structures include three of the four tremors with energy greater than 10^7 J registered during mining of face 3/503 (see Figure 14).

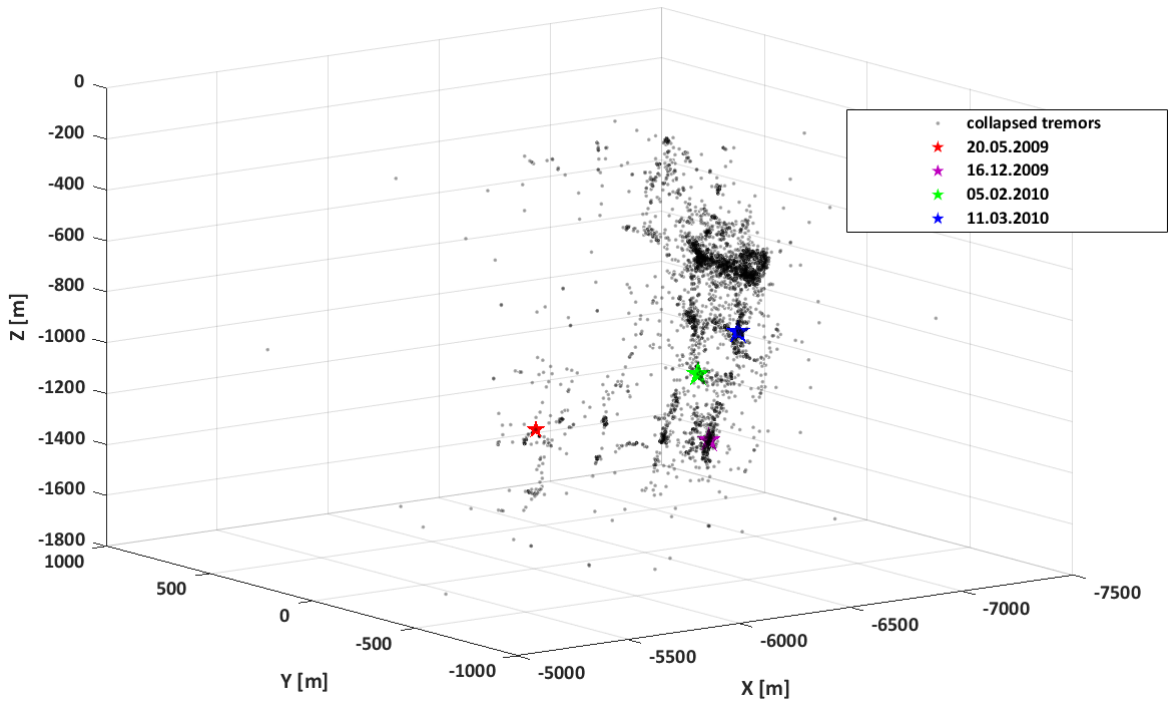

Figure 14. Location of the foci of the four largest tremors recorded during mining of the seam against the backdrop of the emission cloud following relocation.

These tremors are located at relatively great depths, which indicates that they are of mining-tectonic origin rather than being induced by mining activity alone. They form part of the linear structures in the emission cloud isolated in Figure 12, which are located below the shafts surrounding the faces of seams that have been mined.

The above observations suggest that vertical or nearly vertical linear structures identified after collapsing the cloud of phenomena correspond to actual zones of rock mass discontinuity activated during mining. The emission recorded during the mining of face 3/503 activated these faults, leading to a series of numerous tremors with energy emitted over a wide range. In turn, horizontal linear structures located near the exploited seams correspond to the rock mass zones directly affected by the mining of hard coal deposits in the region of the Bytom basin axis. Deeper horizontal structures, which have also been activated by mining and, like vertical structures, occur near the basin axis, may be associated with discontinuities and stress distribution in the synclinal region, as is mentioned by Marcak and Mutke(2013).

7. Summary

The relocation method allows for greater accuracy in identifying the structures associated with seismic zones in the cloud of seismic emission sources. According to the authors of the method, the source cloud after relocation corresponds, statistically speaking, to the original cloud before relocation, in the sense that it provides a picture of the spatial distribution of sources acceptable within the framework of location error. Both distributions clearly differ in their degree of

heterogeneity. After the collapse, this heterogeneity increases significantly and, as a rule, there is a clear tendency towards a concentration within the cloud. They are identified with seismically active zones such as systems of fractures and fissures, faults and areas affected, e.g. by mining activity. Because seismogenic zones are often associated with areas of high stress concentration, collapsing makes it possible to verify certain hypotheses regarding the distribution of tectonic stress in a deformed rock mass.

Imaging of structures based on non-localized locations is in many cases a subjective operation that does not guarantee reproducible results. The collapsing operation makes it possible to reduce the degree of subjectivity when identifying structures and as a consequence increase the reliability of the method itself.

It is important to note that the more numerous the set of registered phenomena and the greater the seismic activity the more effective this method is. In the case of seismic emissions registered in underground mines, the main triggering factor is mining of the deposits. The site where these deposits are mined gradually moves in accordance with the established mining plan. The method described in this article makes a positive result possible if the zones of each seismogenic zone are imaged via at least several dozen phenomena.

Another factor that is key to its success is that it accurately determines ellipsoidal errors of location for individual phenomena. If the location error is very small and the emission is likewise small, the relocation of the sources will be small and the resolution of the point cloud will not improve significantly. In turn, large error ellipsoids, which will overlap to a large extent, which in turn will result in extreme cases in the sources collapsing too intensively into one or a few centers containing most points. As is shown in practice, the best results are achieved when the ellipsoid size is assumed at a confidence level of 99.5%.

The method discussed in this article ensures greater precision when mapping seismogenic zones in a rock mass. As the example presented in this article shows, if used properly, the method allows these zones to be connected with stress concentration sites as well as discontinuities and damaged zones. Compared with other geophysical methods for mapping discontinuities and monitoring dynamic changes in underground mines, seismology supported by appropriately selected processing methods (as shown above) ensures the widest range and satisfactory resolution.

Data

Dataset used for this research are available in IS-EPOS project(https://tcs.ah-epos.eu/#episode:BOBREK).

References

Asanuma, H., Ishimoto, M., Jones, R.H., Phillips, W.S., Niitsuma, H. (2001). A Variation of the Collapsing Method to Delineate Structures Inside a Microseismic Cloud. *Bulletin of the Seismological Society of America*, 91(1), 154-160, http://dx.doi.org/10.1785/0120000063

572 Asanuma, H., Kumano, Y., Izumi, T., Soma, N., Niitsuma, H., Baria, R. (2005). *Monitoring of*
573 *Reservoir Behavior at Soultz HDR Field by Super-Resolution Microseismic Mapping*. Paper
574 presented at Proceedings World Geothermal Congress, Antalya, Turkey.
575 Asanuma, H., Kumano, Y., Niitsuma, H., Wyborn, D., Schanz, U., Haring, M. (2008). *Current*
576 *Status of Microseismic Monitoring Techniques for the Stimulation of HDR/HFR Reservoirs.*
577 Paper presented at Australian Geothermal Energy Conference, Melbourne, Australia.
578 Evernden, J.F. (1969). Precision of epicenters obtained by small numbers of world-wide stations.
579 *Bulletin of the Seismological Society of America*, 59(3), 1365-1398.
580 Fehler, M., House, L., Scott Phillips, W. (1997). Identifying Structures in Clouds of Induced
581 Microseismic Events. *Society of Exploration Geophysicists*.
582 Geiger, L. (1912). Probability method for the determination of earthquake epicenters from the
583 arrival time only. *Bull St Louis Univ* 8, 60–71.
584 Gibowicz, J.S., Kijko, A. (1994). *An Introduction to Mining Seismology.* San Diego: Elsevier
585 Science.
586 Goszcz, A. (1999). *Elementy mechaniki skał oraz tąpania w polskich kopalniach węgla i miedzi.*
587 Kraków:Wydawnictwo Instytutu Gospodarki Surowcami Mineralnymi i Energią PAN.
588 Havskov, J., Ottemoller, L. (2010). *Routine Data Processing in Earthquake Seismology: With*
589 *Sample Data, Exercises and Software*. Springer
590 IS EPOS (2017), Episode: BOBREK, https://tcs.ah-epos.eu/#episode:BOBREK,
591 doi:10.25171/InstGeoph_PAS_ISEPOS-2017-003
592 Jones, R.H., Stewart, R.C. (1997). A method for determining significant structures in a cloud of
593 earthquakes. *Journal of Geophysical Research: Solid Earth*, 102(B4), 8245–8254.
594 https://doi.org/10.1029/96jb03739
595 Kozłowska, M., Orlecka-Sikora, B., Rudziński, Ł., Cielesta, S., Mutke, G. (2016). Atypical
596 evolution of seismicity patterns resulting from the coupled natural, human-induced and
597 coseismic stresses in a longwall coal mining environment. *International Journal of Rock*
598 *Mechanics and Mining Sciences*, 86, 5–15. https://doi.org/10.1016/j.ijrmms.2016.03.024
599 Leśniak, A. (2015). Seismic network configuration by reduction of seismic source location
600 errors. *International Journal of Rock Mechanics and Mining Sciences*, 80, 118-128.
601 https://doi.org/10.1016/j.ijrmms.2015.09.013
602 Leśniak, A., Pszczoła, G. (2008). Combined mine tremors source location and error evaluation in
603 the Lubin Copper Mine (Poland). *Tectonophysics*, 456, 16–27.
604 https://doi.org/10.1016/j.tecto.2007.04.012
605 Li, Y., Hou, G., Hari, K.R., Neng, Y., Lei, G., Tang, Y., Zhou, L., Sun, S., Zheng, C. (2018). The
606 model of fracture development in the faulted folds: The role of folding and faulting. *Marine*
607 *and Petroleum Geology*, 89, 243–251. https://doi.org/10.1016/j.marpetgeo.2017.05.025
608 Marcak, H., Mutke, G. (2013). Seismic activation of tectonic stresses by mining. *Journal of*
609 *Seismology*, 17, 1139–1148. https://doi.org/10.1007/s10950-013-9382-3
610 McGarr, A. (2000). Energy budgets of mining-induced earthquakes and their interactions with
611 nearby stopes. *International Journal of Rock Mechanics and Mining Sciences*, 37, 437-443.
612 https://doi.org/10.1016/s1365-1609(99)00118-5
613 Mosegaard, K., Sambridge, M. (2002). Monte Carlo analysis of inverse problems. *Inverse*
614 *Problems*, 18, R29-R54. https://doi.org/10.1088/0266-5611/18/3/201
615 Phillips, W.S., House, L.S., Fehler, M.C. (1997). Detailed joint structure in geothermal reservoir
616 from studies of induced microearthquake clusters. *Journal of Geophysical Research*,102(B6),
617 11,745-11,763. https://doi.org/10.1029/97JB00762

Rudziński, L., Dębski, W. (2013), Extending the double difference location technique-improving hypocenter depth determination. *Journal of Seismology* 17, 83–94. https://doi.org/10.1007/s10950-012-9322-7

Stec, K. (2009). *Characteristics of the processes taking place at the sources of high energy tremors occurring in the Upper Silesian Coal Basin in Poland – regional character.* Paper presented at 7th International Symposium on Rockbursts and Seismicity in Mines, Dalian, China.

Stec, K. (2007). Characteristics of seismic activity of the Upper Silesian Coal Basin in Poland. *Geophysical Journal International* 168, 757–768. https://doi.org/10.1111/j.1365-246X.2006.03227.x